



Summary

In the realm of wireless power transfer, a burgeoning field characterized by the transmission of electrical energy without physical connectors, our team composed of undergraduate students pursuing a bachelor in electronic engineering, embarked on an ambitious project titled "The Infinite Reflexion Floating Lamp." This project epitomizes the fusion of electromagnetic induction principles and aesthetic innovation. Our project aims to create a visually and technologically sophisticated levitating dodecahedron lamp.

Central to this system are two architectures: the foundational supporting part, and the levitating segment. The supporting part encompasses an advanced levitator, employing permanent repellant magnets coupled with precision-position correction coils. These coils, governed by a feedback mechanism from the Hall effect sensors, ensure stable levitation of the dodecahedron. Additionally, a dedicated wireless power transfer system, comprising a pair of intricately designed coils, facilitates efficient energy transmission to the levitating component.

The levitating part, incorporates a diode bridge with a Buck adept at converting alternating current (AC) to direct current (DC), essential for powering the integrated LEDs. This conversion process is meticulously optimized for maximum efficiency.

Our theoretical framework delves into the nuances of coil sizing and critical coupling in a magnetically coupled resonant wireless power system. Utilizing a refined equivalent circuit model, we analyze the interplay between the transmit and receive coils, focusing on maximizing the system's efficiency through optimal coupling coefficients and quality factors. This analysis is substantiated by extensive simulations conducted via LTSpice, offering insights into the system's electromagnetic behavior and power transfer efficiency.

As we transition from theoretical modeling to empirical validation, our focus pivots towards the construction and testing of a prototype. This phase is critical for assessing the real-world applicability of our design and fine-tuning the system's parameters based on empirical data. Our project serves as a testament of the synergy between technological innovation and artistic design in creating functional yet aesthetically captivating devices.

Table of Contents

Summary	1
Table of Contents	2
1. Introduction	3
2. The Proposed System	3
2.1 The supporting part	4
2.2 The levitating part	4
3. Theoretical Analysis	5
3.1 Theoretical coil sizing	5
3.2 DC/AC Transmitter Coil Conversion	7
3.3 AC/DC Receiver Coil Conversion	8
4. Initial Design	9
5. Simulation and Experimental Results	10
6. Conclusion and Future Work	11
7. References	11

1. Introduction

At the intersection of technological innovation and visual art, our team of undergraduate third-year students in a technological university bachelor's program in electronics embarks on a challenge as bold as it is intriguing. Our project, the "The infinite reflexion floating lamp" pushes the boundaries of creativity, electromagnetism, and wireless energy transfer.



This lamp, taking the form of an infinite dodecahedron, embodies the perfect fusion of aesthetic beauty and cutting-edge engineering. By defying gravity and being powered remotely, it offers a unique visual experience, an interactive work of art that combines the wonder of magnetic levitation with the magic of wireless lighting. Our project aims to showcase our mastery of electromagnetism technologies while igniting the imagination of those who behold it.

Fig. 1 infinite dodecahedron.

Creating a levitating, infinitely mirrored dodecahedron through the application of electromagnetic principles and wireless energy transmission represents a remarkable fusion of science, art, and engineering. This groundbreaking project transcends the boundaries of conventional design and challenges the frontiers of innovation. At its core, this endeavor explores the intricate dance between magnetic fields, geometric precision, and energy transfer, encapsulating the essence of modern technological marvels. By harnessing the power of wireless energy transmission, we not only revolutionize the way we power and control devices, but we also delve into uncharted territory, pushing the boundaries of our understanding of electromagnetic phenomena. The dodecahedron, with its twelve pentagonal faces, is not only a geometric masterpiece but also serves as a canvas for an awe-inspiring visual spectacle. As it hovers in space, the mirrors adorning its surfaces reflect a seemingly infinite expanse of captivating imagery, inviting us to question the very nature of reality. This project is not just an ambitious experiment; it's a journey into the heart of science, art, and human ingenuity, seeking to redefine our relationship with the physical world and the boundless possibilities of electromagnetic technology.

2. The Proposed System

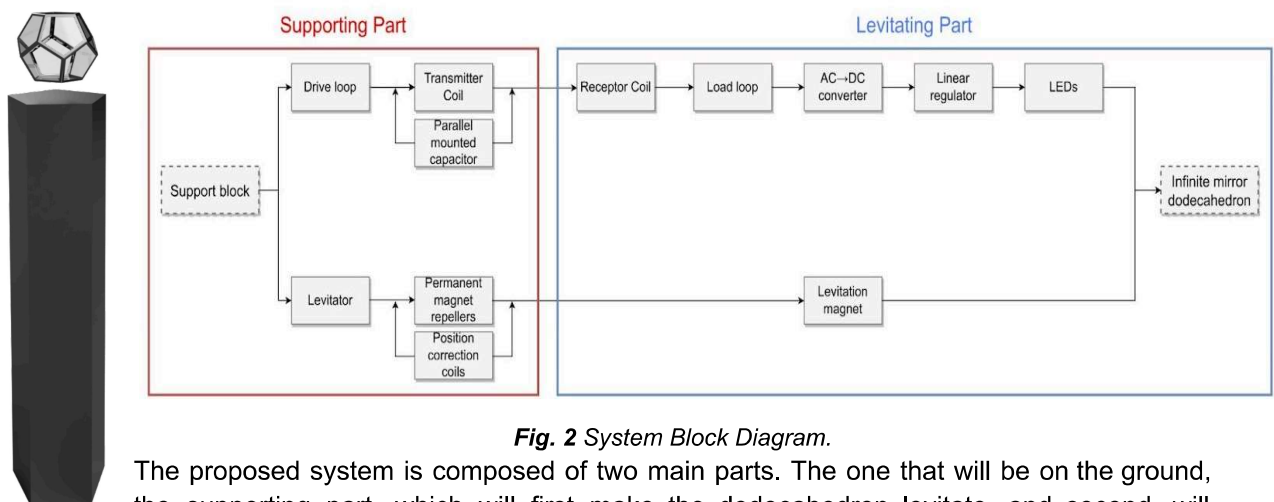


Fig. 2 System Block Diagram.

The proposed system is composed of two main parts. The one that will be on the ground, the supporting part, which will first make the dodecahedron levitate, and second, will transmit a signal to power the dodecahedron's LEDs wirelessly. Then the second main part, the levitating part, features the dodecahedron with its LEDs, and a part stuck to the dodecahedron whose purpose is to be repelled by the levitator's magnetic field and adapt the signal received wirelessly to power the LEDs.

2.1 The supporting part

When considering the entire system, the supportive component exhibits a dual facet. This division involves the segment responsible for levitation and another tasked with wireless power transfer.

Within a preceding and parallel project, we undertook the development and optimization of a device specifically designed for magnet levitation. Termed the "levitator," this apparatus comprises three integral components. Firstly, the permanent repellant magnets generate a magnetic field, facilitating the levitation of our magnet. Following this, the position correction coils come into play, generating magnetic fields to stabilize the levitating magnet. At the core of our arrangement, between the four coils, lie two captors. These captors dutifully relay the microcontroller information regarding the magnet's position, with one captor assigned to the X axis and the other to the Y axis. Subsequently, the microcontroller utilizes this positional data to regulate the coils, thereby ensuring the stable levitation of the magnet.

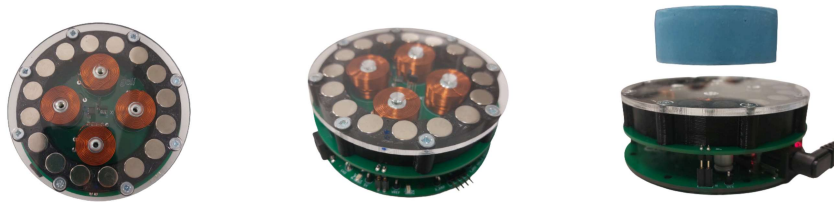


Fig. 3 Levitator.

The subsequent part, responsible for managing wireless power transfer, is a multifaceted subsystem consisting of two distinct coils. These coils operate in tandem, with one serving as a resonator strategically employed to transmit a signal to the levitating segment of the system. A more intricate exploration of the design nuances and specific details pertaining to these coils will be delved into later in this document.

2.2 The levitating part

The levitating part integrates the magnet atop the levitator with the receiving element of the wireless power transfer system. This tandem plays a pivotal role, seamlessly connecting levitation and power reception.

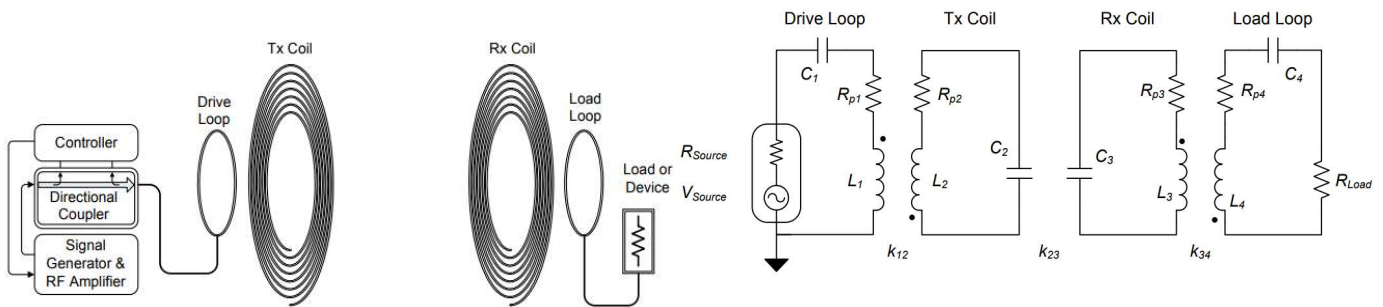
Upon receiving the signal, one coil, acting as a resonator, facilitates the crucial conversion from alternating current (AC) to direct current (DC). This is vital for the LEDs, requiring DC for optimal operation. Precise voltage regulation is a key facet of our design philosophy, ensuring the LEDs receive the exact voltage needed for efficiency and stability.

At the project's core is the dodecahedron—a geometric marvel with a PLA framework, plexiglass faces, and two-way mirrors. Housing strategically placed LEDs, this central structure radiates light through its facets, achieving a visually captivating result. The project harmonizes levitation, wireless power transfer, and LED integration, epitomizing a meticulous blend of functionality and artistic expression.

3. Theoretical Analysis

3.1 Theoretical coil sizing

We have taken on the problem of wireless power transmission with our project. We are developing a system with magnetically connected resonators to do this. A multi-turn spiral coil and a single-turn driving loop make up the transmit antenna. The Tx coil, which stores energy similarly to a discrete LC tank, is excited by the oscillating magnetic field created when the RF amplifier powers the driving loop. Similar operations occur on the receive side, but instead of a power supply, a load is used, and the system is seen by the receive coil as a step-down transformer. The crucial interaction takes place between the two coils, each of which is an LCR tank resonator with a high Q. The transmit and receive coils have a mutual inductance that depends on their geometry and distance from one another, just as the loop and coil are magnetically connected. With this system, we obtain the following circuit diagram, and we can give the equivalent circuit model of the wireless power system, where each of the four antenna elements are modeled as series resonators, which are linked by mutual inductances via coupling coefficients. With this system, we obtain the following circuit diagram, and we can give the equivalent circuit model of the wireless power system, where each of the four antenna elements are modeled as series resonators, which are linked by mutual inductances via coupling coefficients.



(a) **Fig. 4.** Sketch of the magnetically coupled resonant wireless power system consisting of a RF amplifier, on the left, capable of measuring the forward and reflected power. A two element transmitter, made of a signal turn drive loop and high Q coil, wirelessly powers the receiver on the right.
 (b) **Fig. 5.** Equivalent circuit model of the wireless power system. Each of the four antenna elements are modeled as series resonators, which are linked by mutual inductances via coupling coefficients.

The schematic consists of four resonant circuits, linked magnetically by coupling coefficients k_{12} , k_{23} , k_{34} . Starting from the left, the drive loop is excited by a source with finite output impedance, R_{source} . A simple one-turn drive loop can be modeled as an inductor (L_1) with parasitic resistance, R_{p1} . A capacitor (C_1) is added to make the drive loop resonant at the frequency of interest. The transmit coil consists of a multturn air core spiral inductor (L_2), with parasitic resistance (R_{p2}). The geometry of the Tx coil determines its self capacitance which is represented as C_2 . Inductors L_1 and L_2 are connected with coupling coefficient k_{12} ; the receive side is defined similarly. Finally, the transmitter and receiver coils are linked by coupling coefficient, k_{23} . A typical implementation of the system would have the drive loop and Tx coil built into a single device such that k_{12} would be fixed. Similarly, k_{34} would also be fixed. Thus k_{23} is the remaining uncontrolled value which varies as a function of the distances between the transmitter and receiver.

Using the simplified model (fig.5), we can find the current present in each resonant circuit, using Kirchhoff's voltage law. We find the current equations (1), and the coupling coefficient is defined in equation (2).

$$\begin{aligned}
 I_1 \left(R_{Source} + R_{p1} + j\omega L_1 + \frac{1}{j\omega C_1} \right) + j\omega I_2 M_{12} &= V_S \\
 I_2 \left(R_{p2} + j\omega L_2 + \frac{1}{j\omega C_2} \right) + j\omega (I_1 M_{12} - I_3 M_{23}) &= 0 \\
 I_3 \left(R_{p3} + j\omega L_3 + \frac{1}{j\omega C_3} \right) + j\omega (I_4 M_{34} - I_2 M_{23}) &= 0 \\
 I_4 \left(R_{Load} + R_{p4} + j\omega L_4 + \frac{1}{j\omega C_4} \right) + j\omega I_3 M_{34} &= 0
 \end{aligned} \tag{1}$$

$$k_{xy} = \frac{M_{xy}}{\sqrt{L_x L_y}}, \quad 0 \leq k_{xy} \leq 1 \tag{2}$$

Our current goal is to maximize the wireless power system's performance. For that, first, we use the equation critical coupling will be derived by substituting the term for series quality factor and resonant frequency, shown in equation (3), into the transfer function.

$$Q_i = \frac{1}{R_i} \sqrt{\frac{L_i}{C_i}} = \frac{\omega_i L_i}{R_i} = \frac{1}{\omega_i R_i C_i}, \quad \omega_i = \frac{1}{\sqrt{L_i C_i}} \tag{3}$$

Here the "i_{th}" subscript denotes the circuit elements in Fig. 5 for example, i = 1 denotes the elements in the drive loop (L₁, C₁, R_{p1}). Note that the expression for ω_i does not include the damping factor attributable to the resistance in the LCR tank; rather, it represents the free resonant frequency of each loop and coil.

The system is defined as symmetrical for simplicity's sake, with Q_{coil} = Q₂ = Q₃ for the Tx and Rx coil quality factors and Q_{loop} = Q₁ = Q₄ for the Tx and Rx loop quality factors being equal. We will refer to the symmetric loop-to-coil coupling, k₁₂ = k₃₄, as k_{lc} and K₂₃ as k_{cc}. Additionally, we'll assume that R_{source} = R_{load}, R_{p1} << R_{source}, R_{p4} << R_{load}, and that each element's uncoupled resonant frequency is defined as ω₀. Lastly, only the voltage gain derivation at the center frequency ω₀ is shown in the equation for the sake of brevity.

$$\left(\frac{V_{Load}}{V_{Source}} \right)_{|\omega=\omega_0} = \frac{ik_{cc}k_{lc}^2 Q_{coil}^2 Q_{loop}^2}{k_{cc}^2 Q_{coil}^2 + (1 + k_{lc}^2 Q_{coil} Q_{loop})^2} \tag{4}$$

The derivative of (7) is taken with respect to kcc in order to determine the function that predicts the critical coupling point, k_{critical}. When the result is set to zero and kcc is solved for, equation (5) is produced, in which all variables are defined as positive.

$$k_{critical} = \frac{1}{Q_{coil}} + k_{lc}^2 Q_{loop} \tag{5}$$

Here k_{critical} defines the extent of the 'magic regime' as shown in Fig. 6. In order to find magnitude at the critical coupling point, k_{critical} is substituted back into kcc in equation (4). The resulting equation represents the maximum efficiency achievable at the furthest possible operation point before the system becomes under-coupled.

Recall that in order to maximize range, we must minimize k_{critical} because this increases the extent of the 'magic regime', which spans from k_{critical} to 1.0. Examining equation (5) shows that reducing k_{lc} lowers k_{critical} and therefore increases range. However, reducing k_{lc} also reduces efficiency. Indeed, the choice of k_{lc} trades off the efficiency level in the 'magic regime' (height of the V-shaped ridge) vs. the extent of the 'magic regime' (spatial length of V-shaped ridge). Fig. 6 is a plot of this trade off curve, |S₂₁|_{critical} vs k_{critical}, as a function of the common parameter k_{lc}.

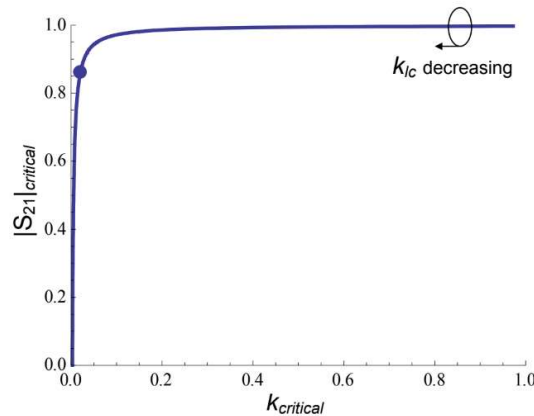


Fig. 6 Efficiency vs critical coupling range: $|S_{21}|_{critical}$ vs. $k_{critical}$ trade off curve as a function of the tuning parameter k_{lc} , with our system's operating point indicated (large dot at $k_{lc}=0.135$).

For system performance, the area under this trade-off curve (FOM) is a helpful measure of merit. A wireless power system with a FOM of unity would be able to deliver power at an infinite range (coupling $\rightarrow 0$) without experiencing any loss.

3.2 DC/AC Transmitter Coil Conversion

In order to supply and excite the emitting coil for energy transfer, we will employ a circuit based on a Wien bridge oscillator^[2]. The oscillator consists of a filtering section that will select the excitation frequency of the coil, as well as an amplification section that will amplify this frequency to sustain the oscillation.

The filtering stage is dimensioned using a second-order bandpass filter (RLC) with a cutoff frequency at 7.65MHz.

Given that $F_c = \frac{1}{2\pi\sqrt{LC}}$, and fixing $C = 1nF$, we obtain $L = \frac{1}{c(2\pi F_c)^2} = 432nH$.

The output

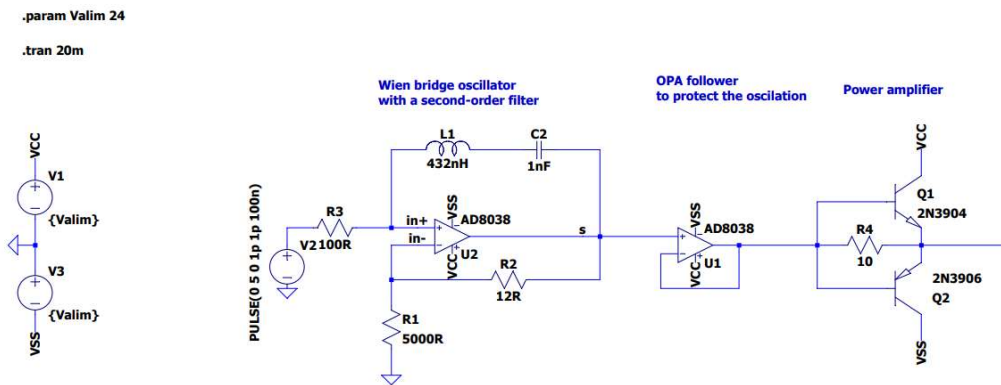


Fig. 7 Oscillator diagram.

By appropriately adjusting the gain of the amplifier to prevent the oscillation from collapsing or saturating the operational amplifier (AOP), we can obtain a quasi-sinusoidal signal at the output. The gain can be adjusted using a potentiometer for an initial prototype. This quasi-sinusoidal signal is fed into an AOP in a follower configuration to isolate it from any disturbances, and is then passed to a current amplifier composed of two bipolar transistors (NPN and PNP) to power the coil.

3.3 AC/DC Receiver Coil Conversion

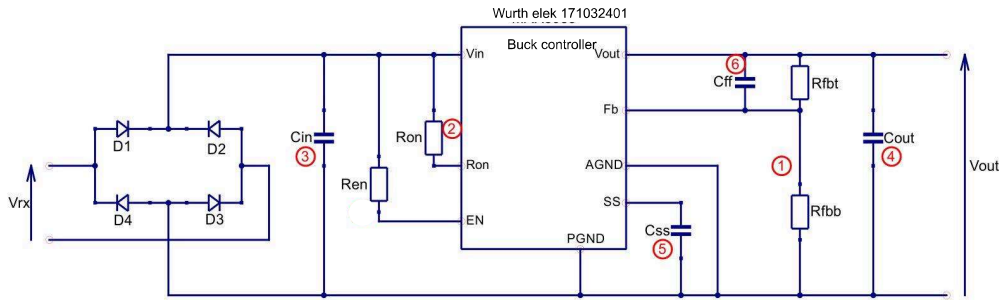


Fig. 8 Rectifier electrical diagram.

For this part the desired output voltage is 24V with a maximum current of 3A, for this we have a diode bridge followed by a buck step-down mounting which is controlled by the wurth elektronik 171032401 component.

1- Ratio feedback resistor :

Output voltage is determined by a divider of two resistors connected between VOUT and ground. The midpoint of the divider is connected to the FB input. The voltage at FB is compared to a 0.8V internal reference. In normal operation an on-time cycle is initiated when the voltage on the FB pin falls below 0.8V. The high-side MOSFET on-time cycle causes the output voltage to rise and the voltage at the FB to exceed 0.8V. As long as the voltage at FB is above 0.8V, on-time cycles will not occur.

The ratio of the feedback resistors for a desired output voltage is:

$$- \frac{R_{FBT}}{R_{FBB}} = \left(\frac{V_{OUT}}{0.8V} \right) - 1$$

These resistors should be chosen from values in the range of 1kΩ to 50kΩ.

We chose $R_{FBT} = 34 \text{ K}\Omega$ and $R_{FBB} = 1.18 \text{ K}\Omega$.

2- Select On-Time Resistor : $R_{ON} = 499 \text{ k}\Omega$.

3- Select Input Capacitor (CIN)

For passive filtering, the following formula is used for the minimum capacitor value:

$$C_{IN_{min}} = \frac{I_{LOAD}}{(2 \times \pi \times f \times V_{RIPPLE})}$$

Taking a charging current of 3A, a nano volt ripple voltage and a cut-off frequency of 20Hz :

$$C_{IN} = 130 \text{ nF}$$

4- Select Output Capacitor (COUT)

$$C_{OUT} = 33\mu\text{F}$$

5- Select Soft-Start Capacitor (CSS)

$$C_{SS} = 4700\text{pF}$$

6- Select Feed Forward Capacitor (CFF)

A feed-forward capacitor CFF is placed in parallel with RFBT which bypasses AC ripple directly to the feedback pin from the output to support the internal ripple generator. This capacitor also affects load step transient response. Its value is usually determined experimentally by load stepping between DCM and CCM conduction modes and adjusting for best transient response and minimum output ripple.

A value of $C_{FF} = 22\text{nF}$ has been practically evaluated as best performing.

4. Initial Design

First of all, we had to design the coil. We are very limited in space as the coils have to fit in the dodecahedron. But for simplicity, we designed the Tx and Rx coil identically and the Drive and Load loop identically.

	external diameter	internal diameter	Number of spires	distance between each spire	wire diameter	inductance	résistance
Loop	20cm	7cm	6	10mm	2.5mm	5.15nH	8.9mΩ
Tx/Rx	9.49cm	9.49cm	1	/	2.5mm	2.28μH	1mΩ

Table. 1 Dimensions of the coils.

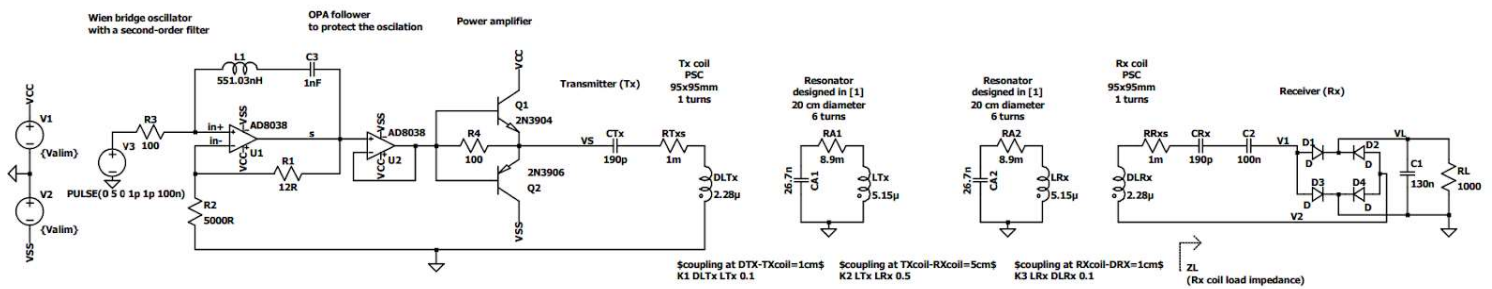


Fig. 9 Electronic system diagram.

We used LTspice to simulate our 4 coils power transfer system, we can now simulate the system to find the power transfer efficiency.

First of all, we wanted to use ANSYS HFSS to calculate the mutual inductance between each coil. Sadly we do not have access to the software and only to the student version which is less powerful and does not allow us to do the calculations needed for a complex system like this one.

So, to find the mutual inductance, we used an experimental method using LTspice. Using this equation :

$$M_{21} = \frac{N_2 \Phi_{21}}{I_1}$$

This allows us to calculate the coupling coefficient between the coils, as we do not have interest in analyzing the mutual inductance between the two loops, between the drive loop and the Rx coil, and between the Tx coil and the load loop, we will not do it. We are interested in the coupling between the drive loop and the Tx, between the Tx and Rx and between the Rx and load loop, note the coupling between drive loop/Rx and between Tx/load loop is going to be the same and stable as the distance between the coils is not going to vary but the other one might vary a bit because the levitation isn't stable.

So we ended up with a coupling of 0.1 for the two couplings and a maximum of 0.3 between Tx and Rx.

5. Simulation and Experimental Results

5.1 Simulation of the DC/AC Transmitter Coil Conversion

We can simulate the oscillator using LTSpice and obtain the following FFTs:

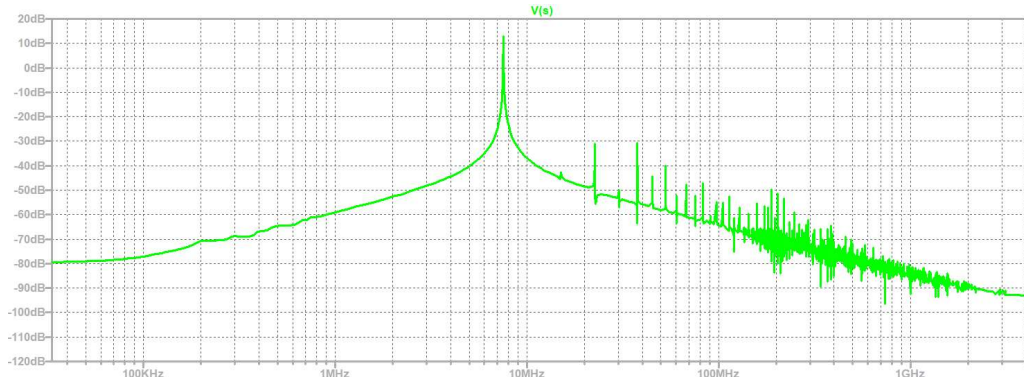


Fig. 10 FFT of the exciting oscillator.

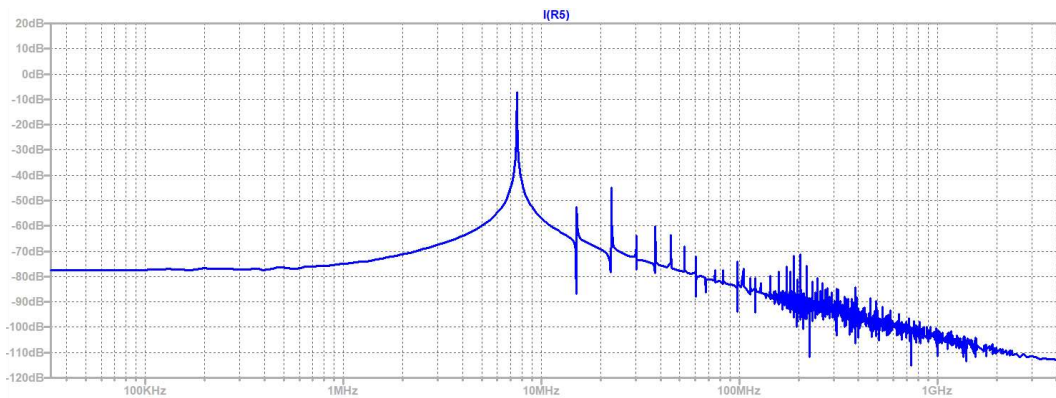


Fig. 11 FFT of the output current.

Thanks to these simulations, we can see the purity of the output voltage and current sinusoids that are very little parasitized.

6. Conclusion and Future Work

As we move forward in our project, having completed a significant portion of the simulations, our focus will shift towards prototyping and verification processes. Utilizing the insights gained from simulations, we'll translate our virtual designs into tangible prototypes, refining practical feasibility and functionality. Verification will play a key role in rigorously testing and validating the system's performance against predefined benchmarks. Our aim is to seamlessly integrate the lessons learned from simulations into the physical prototypes, ensuring the magnetic levitation, wireless power transfer, and LED integration project aligns with our goals of stability and efficiency.

	<i>Items</i>	<i>Quantity</i>	<i>Price</i>	<i>Subtotal</i>
<i>part</i>	magnetic levitation part	1	500€	
	Wireless power transfer part	1	500€	
<i>equipment</i>	Scope and probe	1	lab has	
<i>software</i>	HFSS LTspice	1	/	
Total cost (USD)				1000€

Table. 2 Budget Table.

7. References

[1] WPMDH1302401 / 171032401 Datasheet

<https://www.we-online.com/components/products/datasheet/171032401.pdf>

[2] Wien bridge oscillator

http://electronique.aop.free.fr/AOP_lineaire_NF/24_Wien.html

[3] Alanson P. Sample, David T. Meyer, and Joshua R. Smith, "Analysis, Experimental Results, and Range Adaptation of Magnetically Coupled Resonators for Wireless Power Transfer", June 04,2010, IEEE.